



Surface Science Letters

# Two-dimensional growth of Pd on a thin FeO(1 1 1) film: a physical manifestation of strong metal–support interaction

R. Meyer, M. Bäumer, Sh.K. Shaikhutdinov \*, H.-J. Freund

*Department of Chemical Physics, Fritz-Haber-Institut der Max-Planck-Gesellschaft, Faradayweg 4-6, Berlin 14195, Germany*

Received 9 July 2003; accepted for publication 20 September 2003

## Abstract

Nucleation and growth of palladium vapor deposited on a thin FeO(1 1 1) film grown on a Pt(1 1 1) have been studied by scanning tunneling microscopy (STM). STM data shows that Pd randomly nucleates on the oxide surface and forms two-dimensional islands at sub-monolayer coverages. Annealing to 600 K results in strong metal sintering, thus forming extended Pd(1 1 1) monolayer islands at low coverage, and a thick Pd(1 1 1) film wetting the FeO substrate, at higher Pd coverage. Our data is in agreement with theoretical predictions which indicates this wetting behavior arises from a strong metal–support interaction between Pd and the FeO(1 1 1) film.

© 2003 Elsevier B.V. All rights reserved.

*Keywords:* Growth; Iron oxide; Palladium; Nucleation; Scanning tunneling microscopy; Wetting

Strong metal–support interaction (SMSI) is most generally defined as a close chemical and physical interaction between the metal and support. SMSI was originally developed as an explanation for the decreased chemisorption of CO and H<sub>2</sub> on metal particles when the underlying oxide is reduced and is most notably observed for platinum and palladium particles on titania [1–3]. A well documented physical manifestation of SMSI is the encapsulation of metal particles by the reduced oxide support [3,4].

To gain a deeper understanding of these phenomena, well defined model systems have been

recently employed in which metal is vapor deposited on oxide single crystals or well ordered oxide thin films. Using a variety of techniques including temperature programmed desorption, ion scattering, X-ray photoelectron spectroscopy, scanning tunneling microscopy, and infrared spectroscopy, various research groups have observed reduced CO chemisorption and encapsulation of the metal particles by the reduced support (TiO<sub>x</sub> or CeO<sub>x</sub> for example) [5–11]. Furthermore, Bowker and co-workers revealed a new type of SMSI effect involving the encapsulation of particles by reoxidation of a reduced TiO<sub>2</sub>(1 1 0) support [12].

In addition to encapsulation, the support may strongly influence morphology of the metal deposits and thereby their reactivity, as the morphology of the deposited metal is essentially determined by the metal–support interaction [13].

\* Corresponding author. Fax: +49-30-8413-4105/4101.

*E-mail address:* [shaikhutdinov@fhi-berlin.mpg.de](mailto:shaikhutdinov@fhi-berlin.mpg.de) (Sh.K. Shaikhutdinov).

The nucleation and growth of Pd has been studied previously on many other oxide surfaces as well, including thin films of  $\text{Al}_2\text{O}_3$  [14],  $\text{MgO}$  [15],  $\text{SiO}_2$  [16],  $\text{Cr}_2\text{O}_3$  [17], and single crystal surfaces of  $\text{MgO}(1\ 0\ 0)$  [18],  $\alpha\text{-Al}_2\text{O}_3(0\ 0\ 0\ 1)$  [19],  $\text{ZnO}(0\ 0\ 0\ 1)$  [20] and  $\text{TiO}_2(1\ 1\ 0)$  [21–23]. In some cases, hemispherical [16,21] or even spherical particles [23] were observed, but well faceted hexagonal or trigonal shapes were observed in others [18,22,24]. In all cases, the particles grew three-dimensionally, except for very low Pd coverages [20,21]. In the present Letter, we report on nucleation and growth of palladium deposited on a thin  $\text{FeO}(1\ 1\ 1)$  film. Unlike the results listed above, our data reveals palladium wetting of the oxide film, which we attribute to the strong interaction between Pd and the polar oxide surface.

The experiments were performed in an ultra-high vacuum (UHV) chamber (base pressure below  $10^{-10}$  mbar). Iron and Pd were vapor deposited with commercial evaporators (Focus EFM3). During deposition, the sample was biased with a retarding potential in order to prevent metal ions from being accelerated towards the sample. Deposition rates were calibrated with a quartz microbalance. Oxygen (99.999%, AGA Gas GmbH) was exposed to the samples with a calibrated directional gas doser.

For the  $\text{FeO}(1\ 1\ 1)$  film preparation, about one monolayer (ML) of Fe (99.95%, Advent) was evaporated onto a clean  $\text{Pt}(1\ 1\ 1)$  substrate at 300 K and subsequently oxidized in approximately  $10^{-6}$  mbar  $\text{O}_2$  at 1000 K for 2 min in accordance with the recipes described in Refs. [25–27]. Oxygen was then pumped out at sample temperature below 770 K while cooling the sample. The quality of the  $\text{FeO}$  film was checked by low energy electron diffraction (LEED) and STM prior to Pd deposition.

Palladium (99.99%, Goodfellow) was deposited on the oxide film at 130 K with a deposition rate of approximately  $0.5\ \text{\AA}\ \text{min}^{-1}$ . The pressure during metal depositions never exceeded  $5 \times 10^{-10}$  mbar.

Commercial Pt–Ir tips were used without further cleaning. Typical tunneling conditions generally fell within ranges of 2–200 mV and 0.5–5 nA, with the observed features independent of bias polarity. All STM images presented in the paper were taken at room temperature.

Fig. 1a presents a typical large scale STM image of a clean  $\text{FeO}$  film, which shows wide flat terraces separated by steps of  $\sim 2.3\ \text{\AA}$  in height corresponding to monoatomic steps of  $\text{Pt}(1\ 1\ 1)$  underneath the film. The terraces exhibit a Moiré pattern with a  $\sim 26\ \text{\AA}$  periodicity and an atomic structure

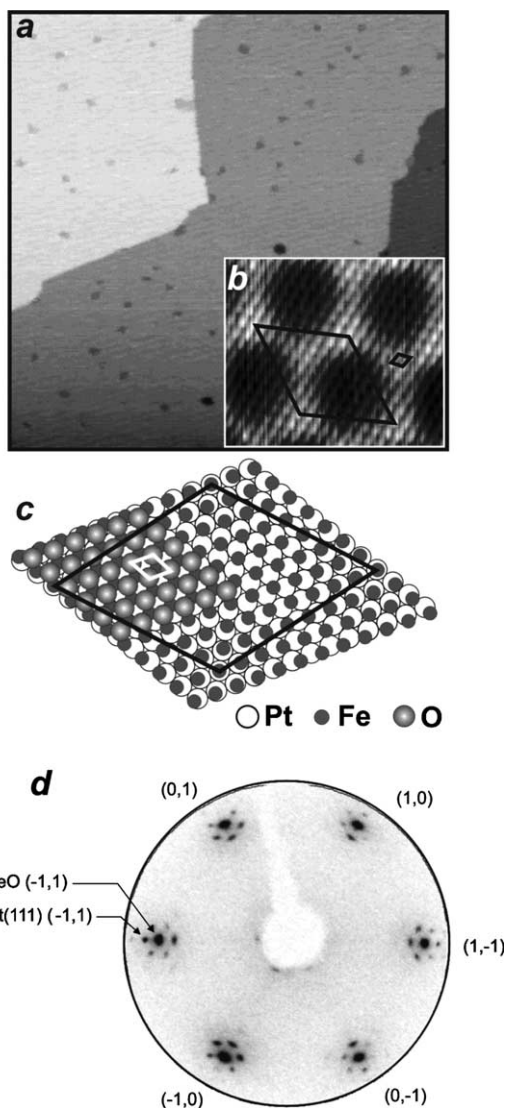


Fig. 1. (a) STM image (size:  $150 \times 150\ \text{nm}^2$ ) of the  $\text{FeO}(1\ 1\ 1)$  film grown on  $\text{Pt}(1\ 1\ 1)$ . Image (b) resolves a Moiré pattern formed due to a mismatch of the  $\text{FeO}(1\ 1\ 1)$  layer with respect to the  $\text{Pt}(1\ 1\ 1)$  surface underneath as depicted in model (c) as suggested in [28]. The unit cells are indicated. Satellite spots arise in the diffraction pattern as a result of the Moiré as shown in (d).

with a  $\sim 3$  Å periodicity as shown in Fig. 1b. The structural model of the FeO overlayer is depicted in Fig. 1c as suggested in [28]. Fig. 1d, shows a typical LEED pattern exhibiting the principal spots from Pt(1 1 1), FeO(1 1 1) as well as satellite spots arising from the Moiré structure.

There are some small domains of 10–30 Å in size and 1 Å in depth, which can be observed on the FeO terraces as holes in the oxide film (see Fig. 1a). The number of such holes is very small ( $\approx 2 \times 10^{10}$  cm<sup>-2</sup>) and totally they cover less than 0.01 ML. For the largest of these holes, the  $c(2 \times 2)$  structure with respect to Pt(1 1 1)-(1  $\times$  1) has been resolved (not shown here). Therefore, we have assigned them to the  $c(2 \times 2)$ -O/Pt(1 1 1) surface formed due to oxy-

gen re-adsorption as the sample cools following the oxidation step. Their presence depends on the amount of iron deposited prior to oxidation. In the case of iron deposition greater than 1 ML, islands of a few angstroms in height with ill-defined structure are found attached to the terrace steps. Such defects (holes or islands) are formed primarily because the amount of iron cannot be precisely deposited to form a perfect FeO monolayer film.

Deposition of  $\sim 0.1$  Å (nominal thickness) of Pd on FeO at 130 K results in a random distribution of the particles of 3–4 nm in size with an apparent height of 2.3 Å (or 1 ML of Pd) as shown in Fig. 2a. No preferential decoration of terraces, steps, or holes is observed as shown in the inset.

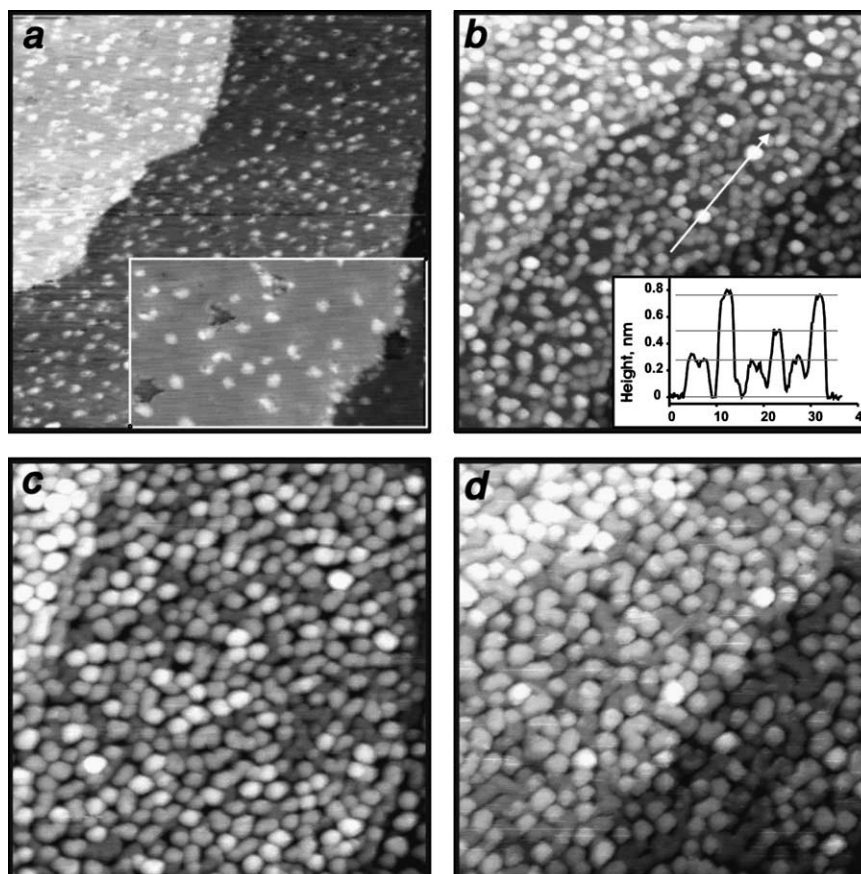


Fig. 2. STM images of Pd deposited on FeO(1 1 1) at 130 K at different Pd coverages: (a) 0.1 Å, (b) 1 Å, (c) 2 Å, and (d) 5 Å. Particles increase in size, with their heights increasing in a “layer-by-layer” mode up to the 4 layer as observed in (d). All images are  $100 \times 100$  nm<sup>2</sup>. The inset in (a) shows the lack of preferential nucleation (size  $35 \times 20$  nm). Inset in (b) shows the surface topography over the line as indicated (scan proceeds from left to right in the direction indicated by the arrow).

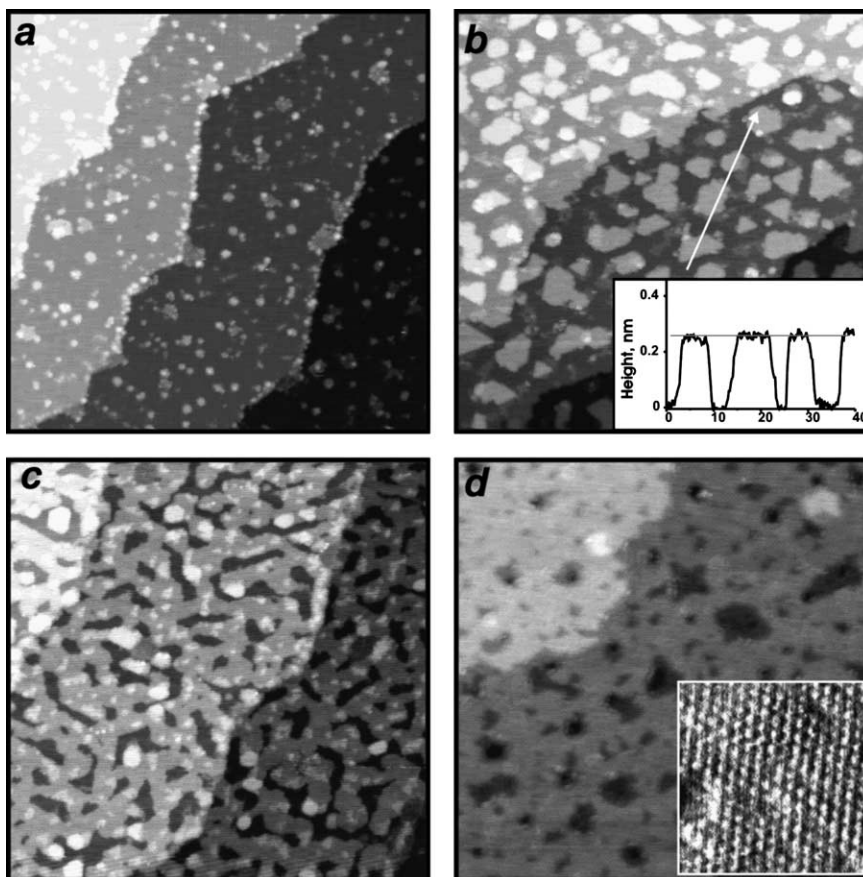


Fig. 3. STM images of Pd deposited on FeO(111) at 130 K and annealed to 600 K at different Pd coverages: (a) 0.1 Å, (b) 1 Å, (c) 2 Å, and (d) 5 Å. Pd deposits strongly sinter upon heating, thus forming extended monolayer islands (b), first (c) and second (d) layers of Pd on FeO. (All images are  $100 \times 100 \text{ nm}^2$ .) Inset in (b) shows the surface topography over the line as indicated (scan proceeds from left to right in the direction indicated by the arrow). The inset in (d) shows the Pd(111) surface of the second layer of Pd exhibiting the “bulk” lattice constant (size  $4 \times 4 \text{ nm}^2$ ).

As shown in Fig. 2b–d, increasing the Pd coverage essentially results in increasing the size of the islands. The islands are mostly flat and exhibit the height multiple of  $\sim 2.3 \text{ \AA}$  as shown in the inset of Fig. 2b. The lateral dimensions of the Pd deposits greatly exceed their heights. This implies a quasi-two-dimensional (2-D) growth mode of Pd on FeO(111) even for relatively high palladium coverages.

Campbell and co-workers have previously shown that 2D growth of metals on oxides at low coverages may occur due to kinetic limitations. However, with increased coverage or temperature,

the deposits irreversibly thicken and three-dimensional particles are formed [29,30]. This type of behavior has been observed for small palladium particles on other metal oxide supports [17,20,21].

In contrast, Fig. 3 shows that annealing of Pd on FeO(111) to 600 K leads to strong particle coalescence and the formation of *monolayer* islands (confirmed by line scans as shown in the inset of Fig. 3b). The islands become much larger and exhibit triangular and/or hexagonal shape at a coverage of 1 Å (Fig. 3b). For a 2 Å-thick Pd overlayer, the first layer is nearly complete and the second layer starts to grow (Fig. 3c). Finally, for a 5 Å coverage, the

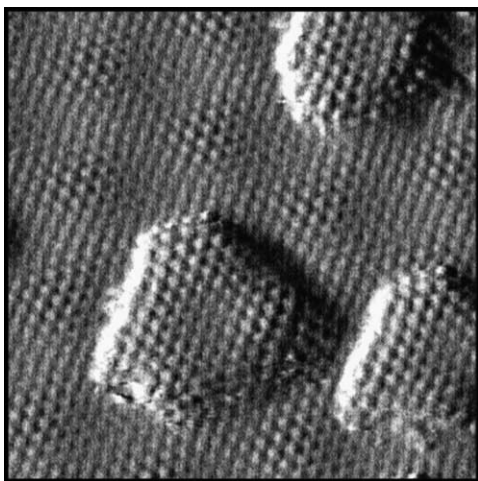


Fig. 4. High-resolution STM image of extended Pd monolayer islands formed after annealing to 600 K. The Pd coverage is  $\sim 1$  Å. The image is presented with differentiated contrast. The image size  $12 \times 12$  nm<sup>2</sup>. Tunneling conditions:  $V = 2$  mV,  $J = 5$  nA.

second layer is formed, with holes of one Pd layer in depth being observed on the terraces (Fig. 3d).

Fig. 4 shows an atomically resolved STM image of extended Pd islands. The image clearly shows Pd(111) islands matching the underlying FeO(111) support. In addition, the surface topology of the Pd islands also exhibits a long-range modulation similar to the Moiré pattern observed on the bare oxide surface. In fact, based on a registry analysis of the high-resolution STM images and with the help of supporting theoretical calculations, we have determined that Pd adsorbs on top of oxygen ions [31]. We believe this phenomena in which the atoms of the metal are in perfect registry with the underlying support is a physical illustration of the strength of the metal–support interaction.

As a result of this unusual epitaxial relationship, spot profile analysis (SPA) of the LEED patterns at sub-monolayer Pd coverages revealed no additional diffraction spots beyond those attributed to the FeO(111)/Pt(111) interface. As the lattice constant of the FeO(111) surface, as measured by Ritter et al. [27], is found to be about 3.1 Å, is 12% larger than for Pd(111) ( $= 2.76$  Å), this implies that the Pd–Pd distance within Pd islands

on FeO is in fact greatly expanded as compared to bulk palladium. Therefore, the metal–support interaction must be sufficiently strong to overcome the large strain induced by the lateral expansion of the extended Pd(111) monolayer islands.

Additional SPA LEED measurements for the annealed 5 Å-thick Pd overlayer have revealed a lattice constant of 2.77 Å i.e., equal to that for a Pd(111) crystal with a simultaneous loss of all diffraction spots characteristic for the FeO(111)/Pt(111) interface. Atomically resolved STM images confirmed that lattice constant of the second Pd layer is indeed  $\sim 2.8$  Å, as shown in the inset of Fig. 3d. Therefore, we can conclude that the annealed Pd film of two atomic layers thick already exhibits the native Pd(111) crystalline surface. It seems likely that the Pd(111) monolayer transforms into the “bulk” Pd(111) film at increasing coverages above 1 ML in order to reduce stress deformations arising due to the lattice mismatch between Pd(111) and FeO(111).

The wetting behavior which we observe for Pd on FeO(111) is rather unusual for transition metals supported on oxide surfaces. Indeed, three-dimensional growth is seen in all systems studied to date [32]. This observation is generally rationalized on the basis that in most metal–metal oxide systems the surface energy of the metal is much greater than the surface energy of the metal oxide. The surface energies of Pd(111) and FeO are found to be  $\sim 1.9$  J m<sup>-2</sup> [33] and  $\sim 0.7$  J m<sup>-2</sup> [34] respectively. Therefore assuming that the interface energy is small, one expects Pd to grow three-dimensionally.

The Pd/FeO(111) system becomes even more intriguing when compared to the behavior of gold on the FeO film. Since gold has a lower surface energy than palladium ( $\sim 1.3$  J m<sup>-2</sup> for Au(111) [33]), one might expect gold to possess strong wetting behavior also. However, gold exhibits a more three-dimensional growth mode [35].

One may argue that the wetting of Pd on FeO could be a unique consequence of the interaction of the metal particles with the thin film as opposed to the bulk phase of FeO. However, Goniakowski and Noguera have recently predicted wetting behavior for Pd deposited on MgO(111) (which shares the same rock salt structure as FeO) [36].

They have calculated that the polar instability of the MgO(1 1 1) face is quenched by metal deposition as a result of charge transfer from the deposited metal (Pd) to the oxygen of the underlying oxide [37]. Upon addition of Pd on oxygen terminated MgO(1 1 1), the calculated charge on O shifted from  $-0.47$  to  $-0.73$ , which is closer to the value for oxygen in the bulk ( $-0.88$ ), thereby stabilizing the MgO(1 1 1) surface, while at the same time, Pd assumes a small positive charge (0.26). Furthermore, Goniakowski and Noguera calculated that significant hybridization between Pd and O orbitals occurs, which also acts to stabilize the polar MgO(1 1 1) surface. Although this electronic effect is admittedly different from that in traditional SMSI, in which a charge transfer occurs from the support to the deposited metal (and thus making Pd or Pt more noble) [3], we attribute this wetting to a consequence of the strong interaction between Pd and (1 1 1) surfaces of rock salt oxides described above. Goniakowski and Noguera's calculations also confirm a lower adhesion energy between gold and MgO(1 1 1) [37], due to lack of electronic interaction between gold and oxygen, which matches our observation of a 3-D growth mode even for low coverages of Au on FeO(1 1 1).

In summary, we have studied nucleation and growth of palladium vapor deposited on a thin FeO(1 1 1) film grown on a Pt(1 1 1) single crystal by STM. Data show that Pd exhibits non-preferential nucleation on the oxide surface and grows quasi-two-dimensionally at room temperature. Annealing to 600 K results in Pd wetting of the FeO film thus forming extended Pd(1 1 1) monolayer islands and a thick Pd(1 1 1) film at higher coverages. This wetting appears to be a physical manifestation of a strong metal-support interaction between Pd and the FeO(1 1 1) film in agreement with theoretical predictions for metals on the (1 1 1) surfaces of rock salt oxide crystals.

### Acknowledgements

This work was supported by Fonds der Chemischen Industrie. RM thanks the Alexander von Humboldt Foundation for a fellowship.

### References

- [1] S.J. Tauster, S.C. Fung, *J. Catal.* 55 (1978) 29.
- [2] S.J. Tauster, S.C. Fung, R.L. Garten, *J. Am. Chem. Soc.* 100 (1978) 170.
- [3] G.L. Haller, D.E. Resasco, *Adv. Catal.* 36 (1989) 173.
- [4] R.T.K. Baker, E.B. Prestridge, R.L. Garten, *J. Catal.* 59 (1979) 293.
- [5] O. Dulub, W. Hebenstreit, U. Diebold, *Phys. Rev. Lett.* 84 (2000) 3646.
- [6] T. Madey, F. Pesty, H.P. Steinruck, *Surf. Sci.* 339 (1995) 83.
- [7] M. Bowker, P. Stone, R. Bennett, N. Perkins, *Surf. Sci.* 497 (2002) 155.
- [8] R.A. Bennett, C.L. Pang, N. Perkins, R.D. Smith, P. Morrall, R.I. Kvon, M. Bowker, *J. Phys. Chem. B* 106 (2002) 4688.
- [9] T. Suzuki, R. Souda, *Surf. Sci.* 448 (2000) 33.
- [10] J. Evans, B.E. Hayden, G. Lu, *Surf. Sci.* 360 (1996) 61.
- [11] D.R. Mullins, K.Z. Zhang, *Surf. Sci.* 513 (2002) 163.
- [12] R.A. Bennett, P. Stone, M. Bowker, *Catal. Lett.* 59 (1999) 994.
- [13] A.Y. Stakheev, L.M. Kustov, *Appl. Catal. A* 188 (1999) 3.
- [14] M. Bäumer, H.-J. Freund, *Prog. Surf. Sci.* 61 (1999) 127.
- [15] C. Xu, W.S. Oh, G. Liu, D.Y. Kim, D.W. Goodman, *J. Vac. Sci. Technol. A* 15 (1997) 1261.
- [16] J.B. Giorgi, T. Schroeder, M. Baumer, H.-J. Freund, *Surf. Sci.* 498 (2002) L71.
- [17] K. Wolter, H. Kuhlenbeck, H.-J. Freund, *J. Phys. Chem. B* 106 (2002) 6723.
- [18] C.R. Henry, C. Chapon, C. Duriez, S. Giorgio, *Surf. Sci.* 253 (1991) 177.
- [19] C.L. Pang, H. Raza, S.A. Haycock, G. Thornton, *Surf. Sci.* 460 (2000) L510.
- [20] H. Jacobs, W. Mokwa, D. Kohl, G. Heiland, *Surf. Sci.* 160 (1985) 217.
- [21] C. Xu, X. Lai, G.W. Zajac, D.W. Goodman, *Phys. Rev. B* 56 (1997) 13464.
- [22] P. Stone, R.A. Bennett, S. Poulston, M. Bowker, *Surf. Sci.* 433 (1999) 501.
- [23] M.J.J. Jak, C. Konstapel, A. Van Kreuningen, J. Verhoeven, J.W.M. Frenken, *Surf. Sci.* 457 (2000) 295.
- [24] K.H. Hansen, T. Worren, S. Stempel, E. Laegsgaard, M. Baumer, H.-J. Freund, F. Besenbacher, I. Stensgaard, *Phys. Rev. Lett.* 83 (1999) 4120.
- [25] G.H. Vurens, M. Salmeron, G.A. Somorjai, *Surf. Sci.* 201 (1988) 129.
- [26] G.H. Vurens, V. Maurice, M. Salmeron, G.A. Somorjai, *Surf. Sci.* 268 (1992) 170.
- [27] M. Ritter, W. Ranke, W. Weiss, *Phys. Rev. B* 57 (1998) 7240.
- [28] H.C. Galloway, J.J. Benitez, M. Salmeron, *J. Vac. Sci. Technol. A* 12 (1994) 2302.
- [29] K.H. Ernst, A. Ludviksson, R. Zhang, J. Yoshihara, C.T. Campbell, *Phys. Rev. B* 47 (1993) 13782.

- [30] C.T. Campbell, A.W. Grant, D.E. Starr, S.C. Parker, V.A. Bondzie, *Top. Catal.* 14 (2001) 43.
- [31] S. Shaikhutdinov, R. Meyer, D. Lahav, M. Bäumer, T. Klüner, H.-J. Freund, *Phys. Rev. Lett.* 91 (2003) 076102.
- [32] C.T. Campbell, *Surf. Sci. Rep.* 27 (1997) 1.
- [33] L. Vitos, A.V. Ruban, H.L. Skriver, J. Kollar, *Surf. Sci.* 411 (1998) 186.
- [34] S.H. Overbury, P.A. Bertrand, G.A. Somorjai, *Chem. Rev.* 75 (1975) 547.
- [35] Sh. Shaikhutdinov, R. Meyer, M. Naschitzki, M. Bäumer, H.-J. Freund, *Catal. Lett.* 86 (2003) 211.
- [36] J. Goniakowski, C. Noguera, *Phys. Rev. B* 60 (1999) 16120.
- [37] J. Goniakowski, C. Noguera, *Phys. Rev. B* 66 (2002) 085417.